

---

# Fearless Stochasticity in Expectation Propagation

---

**Jonathan So**  
University of Cambridge  
js2488@cam.ac.uk

**Richard E. Turner**  
University of Cambridge  
ret26@cam.ac.uk

## Abstract

Expectation propagation (EP) is a family of algorithms for performing approximate inference in probabilistic models. The updates of EP involve the evaluation of moments—expectations of certain functions—which can be estimated from Monte Carlo (MC) samples. However, the updates are not robust to MC noise when performed naively, and various prior works have attempted to address this issue in different ways. In this work, we provide a novel perspective on the moment-matching updates of EP; namely, that they perform natural-gradient-based optimisation of a variational objective. We use this insight to motivate two new EP variants, with updates that are particularly well-suited to MC estimation; they remain stable and are most sample-efficient when estimated with just a single sample. These new variants combine the benefits of their predecessors and address key weaknesses. In particular, they are easier to tune, offer an improved speed-accuracy trade-off, and do not rely on the use of debiasing estimators. We demonstrate their efficacy on a variety of probabilistic inference tasks.

## 1 Introduction

Expectation propagation (EP) [33, 36] is a family of algorithms that is primarily used for performing approximate inference in probabilistic models [7, 8, 9, 10, 13, 15, 17, 16, 18, 19, 20, 21, 25, 26, 27, 28, 31, 32, 34, 35, 37, 40, 43, 44, 46, 47, 48], although it can be used more generally for approximating certain kinds of functions and their integrals [11].

EP involves the evaluation of moments—expectations of certain functions—under distributions that are derived from the model of interest. EP is usually applied to models for which these moments have convenient closed-form expressions or can be accurately estimated using deterministic methods. Moments can also be estimated using Monte Carlo (MC) samples, significantly expanding the set of models EP can be applied to; however, the updates of EP are not robust to MC noise when performed naively, and various prior works have attempted to address this issue in different ways [14, 44, 47].

In this work we provide a novel perspective on the moment-matching updates of EP; namely, that they perform natural-gradient-based optimization of a variational objective (Section 3). We use this insight to motivate two new EP variants,  $EP-\eta$  (Section 3.2) and  $EP-\mu$  (Section 3.3), with updates that are particularly well-suited to MC estimation, remaining stable and being most sample-efficient when estimated with just a single sample. These new variants combine the benefits of their predecessors and address key weaknesses. In particular, they are easier to tune, offer an improved speed-accuracy trade-off, and do not rely on the use of debiasing estimators. We demonstrate their efficacy on a variety of probabilistic inference tasks (Section 4).

## 2 Background

In this section, we first introduce the problem setting. We then give an overview of EP, followed by a discussion of issues related to sampled estimation of EP updates.

Let  $\mathcal{F}$  be the tractable, minimal exponential family of distributions (see Appendix A), defined by the statistic function  $s(\cdot)$  with respect to base measure  $\nu(\cdot)$ . Let  $\Omega$ ,  $\mathcal{M}$ ,  $A(\cdot)$  and  $A^*(\cdot)$  denote the natural domain, mean domain, log partition function, and negative entropy function of  $\mathcal{F}$ , respectively.

Let  $p_0$  be the member of  $\mathcal{F}$  with natural parameter  $\theta_0$ , so that  $p_0(z) = \exp(\theta_0^\top s(z) - A(\theta_0))$ <sup>1</sup>, and assume that a distribution of interest  $p^*$ , the *target distribution*, has a density of the form

$$p^*(z) \propto p_0(z) \prod_{i=1}^m \exp(\ell_i(z)). \quad (1)$$

In Bayesian inference settings,  $p^*$  would be the posterior distribution over parameters  $z$  given some observed data  $\mathcal{D}$ , where  $p_0$  may correspond to a prior distribution, and  $\{\ell_i(z)\}_i$  to log-likelihood terms given some partition of  $\mathcal{D}$ .<sup>2</sup> However, we consider the more general setting in which the target distribution is simply a product of factors; note that we can assume form (1) without loss of generality if we allow  $p_0$  to be improper. The inference problem typically amounts to evaluating quantities derived from the normalised density  $p^*(z)$ , such as samples, summary statistics, or expectations of given functions. In some special cases, these quantities can be computed exactly, but this is not feasible in general, and approximations must be employed.

## 2.1 Expectation propagation (EP)

Given a target distribution density of form (1), EP aims to find an approximation  $p \in \mathcal{F}$  such that

$$p(z) \propto p_0(z) \prod_i \exp(\lambda_i^\top s(z)) \approx p^*(z). \quad (2)$$

By assumption  $\mathcal{F}$  is tractable, and so provided that  $(\theta_0 + \sum_{i=1}^m \lambda_i) \in \Omega$ ,  $p$  is a tractable member of  $\mathcal{F}$ . Each factor  $\exp(\lambda_i^\top s(z))$  is known as a *site potential*, and can be roughly interpreted as a  $\mathcal{F}$ -approximation to the  $i$ -th *target factor*,  $\exp(\ell_i(z))$ .<sup>3</sup>  $\lambda_i$  is known as the  $i$ -th *site parameter*.

**Variational problem** EP, and several of its variants [14, 21, 33], can be viewed as solving a variational problem which we now introduce following the exposition of Hasenclever et al. [14].

Let the  $i$ -th *locally extended family*, denoted  $\mathcal{F}_i$ , be the exponential family defined by the statistic function  $s_i(z) = (s(z), \ell_i(z))$  with respect to base measure  $\nu(\cdot)$ . Let  $\Theta_i$ ,  $\mathcal{M}_i$  and  $A_i(\cdot)$  denote the natural domain, mean domain, and log partition function of  $\mathcal{F}_i$ , respectively. Note that a member of  $\mathcal{F}_i$  roughly corresponds to a distribution whose density is the (normalised) product of a member of  $\mathcal{F}$  with the  $i$ -th target factor raised to a power. Unlike  $\mathcal{F}$ , we do not assume  $\mathcal{F}_i$  is minimal.

Fixed points of EP correspond to the solutions of the saddle-point problem

$$\begin{aligned} & \max_{\{\theta_i \in \Omega\}_i} \min_{\{\lambda_i\}_i} L(\theta_1, \dots, \theta_m, \lambda_1, \dots, \lambda_m), \text{ where} \\ L(\theta_1, \dots, \theta_m, \lambda_1, \dots, \lambda_m) &= A\left(\theta_0 + \sum_i \lambda_i\right) + \sum_i \beta_i [A_i((\theta_i - \beta_i^{-1} \lambda_i, \beta_i^{-1})) - A(\theta_i)]. \end{aligned} \quad (3)$$

At a solution to (3), the EP approximation is given by (2). The hyperparameters  $\{\beta_i\}_i$  control the characteristics of the approximation, and correspond to the power parameters of power EP.

**EP updates** EP [33, 36], power EP [30] and double-loop EP [21], can all be viewed as alternating between some number ( $\geq 1$ ) of *inner updates* to decrease  $L$  with respect to  $\{\lambda_i\}_i$ , with an *outer update* to increase  $L$  with respect to  $\{\theta_i\}_i$  [14, 22]. EP is not typically presented in this way, but by doing so we will be able to present a unified algorithm that succinctly illustrates the relationship between the different variants. The inner and outer updates are given by

$$\textbf{Inner update: } \lambda_i \leftarrow \lambda_i - \alpha \left( \theta_0 + \sum_j \lambda_j - \nabla A^*(\mathbb{E}_{p_i(z)}[s(z)]) \right), \quad (4)$$

$$\textbf{Outer update: } \theta_i \leftarrow \theta_0 + \sum_j \lambda_j, \quad (5)$$

<sup>1</sup>We use e.g.  $p$  to refer to a distribution, and  $p(\cdot)$  or  $p(z)$  for its density, throughout.

<sup>2</sup>Going forward, we assume  $i$  and  $j$  to be taken from the index set  $\{1, \dots, m\}$  unless otherwise specified.

<sup>3</sup>This interpretation is not precise, since it is not necessarily the case that  $\lambda_i \in \Omega$ .

where  $p_i \in \mathcal{F}_i$  denotes the  $i$ -th *tilted distribution*, with density

$$p_i(z) \propto p_0(z) \exp\left((\theta_i - \beta^{-1}\lambda_i)^\top s(z) + \beta^{-1}\ell_i(z)\right). \quad (6)$$

The hyperparameter  $\alpha$  controls the level of damping, which is used to aid convergence. An undamped inner update (with  $\alpha = 1$ ) can be seen as performing *moment matching* between  $p$  and  $p_i$ . The inner updates can be performed either serially (over  $i$ ) or in parallel. In this work we assume they are applied in parallel, but the ideas presented can easily be extended to the serial case. Heskes and Zoeter [22] showed that (4) follows a decrease direction in  $L$  with respect to  $\lambda_i$ , and so is guaranteed to decrease  $L$  when  $\alpha$  is small enough. See Appendix B for a derivation of the inner update. When  $\{\lambda_i\}_i$  are at a partial minimum of  $L$  (for fixed  $\{\theta_i\}_i$ ), the outer update performs an exact partial maximisation of the primal form of the variational problem; see Hasenclever et al. [14] for details.

**Unified EP algorithm** The double-loop EP algorithm of Heskes and Zoeter [21] repeats the inner update to convergence before performing each outer update, which ensures convergence of the overall procedure. The usual presentation of EP combines (4) and (5) into a single update in  $\lambda_i$ ; however, Jylänki et al. [27] observed that it can also be viewed as performing double-loop EP with just a single inner step per outer update (which is not guaranteed to converge in general). By taking this viewpoint, we are able to present EP, power EP, and their double-loop counterparts as a single algorithm, presented in Algorithm 1. Note that the dependence on  $\{\beta_i\}_i$  comes through the definition of  $p_i(\cdot)$ .

---

**Algorithm 1** EP ( $\beta_i=1, n_{\text{inner}}=1$ ), power EP ( $\beta_i \neq 1, n_{\text{inner}}=1$ ), and their double-loop variants ( $n_{\text{inner}} > 1$ )

---

**Require:**  $\mathcal{F}$ ,  $\theta_0$ ,  $\{\beta_i\}_i$ ,  $\{\ell_i(z)\}_i$ ,  $\{\lambda_i\}_i$ ,  $n_{\text{inner}}$ ,  $\alpha$   
**while** not converged **do**  
     $\theta_i \leftarrow \theta_0 + \sum_j \lambda_j$  for  $i = 1$  to  $m$   
    **for** 1 to  $n_{\text{inner}}$  **do**  
        **for**  $i = 1$  to  $m$  *in parallel* **do**  
             $\lambda_i \leftarrow \lambda_i - \alpha \left( \theta_0 + \sum_j \lambda_j - \nabla A^*(\mathbb{E}_{p_i(z)}[s(z)]) \right)$   
    **return**  $\{\lambda_i\}_i$

---

We can think of "exact" double-loop EP as corresponding to  $n_{\text{inner}} = \infty$ , with the inner loop exiting only once some convergence criteria has been satisfied. In practice, a truncated inner loop is often used by setting  $n_{\text{inner}}$  to some small number [14, 27]. Upon convergence of Algorithm 1, the approximation  $p(z) \approx p^*(z)$  is given by (2). Going forwards we will refer to the family of algorithms encompassed by Algorithm 1 simply as EP.

**Stochastic moment estimation** EP is typically applied to models for which the updates either have closed-form expressions, or can be accurately estimated using deterministic numerical methods. However, as update (4) only depends on the target distribution through expectations under the tilted distributions, this suggests that updates could also be performed using *sampled* estimates of those expectations. By using MC methods to estimate the tilted distribution moments, EP can be applied in a black-box manner, dramatically expanding the space of models it can be applied to. Instead of performing a single large sampling task—as would be required by applying MC methods directly—EP can instead solve several simpler ones, gaining significant computational advantages [14, 44, 47]. Unfortunately, when performed naively, update (4) is not robust to MC noise. This is because the moment estimates are converted to the natural (site) parameter space by mapping through  $\nabla A^*(\cdot)$ , which is not linear in general, and so MC noise in the estimates leads to biased updates of  $\lambda_i$ .

### 3 Fearlessly stochastic EP algorithms

In this section we show an equivalence between the moment-matching updates of EP and natural gradient descent (NGD). We use this view to motivate two new EP variants which have several advantages when updates are estimated using samples. We conclude with a review of related work.

#### 3.1 Natural gradient view of EP

Several EP variants—EP, power EP, double loop EP, SNEP, and the new ones to follow—differ only in how they perform the *inner* optimisation in (3) with respect to  $\{\lambda_i\}_i$ . The optimisation can be

viewed as one with respect to the  $m + 1$  distributions  $p, p_1, \dots, p_m$ , which are jointly parameterised by  $\{\lambda_i\}_i$  [14]. Natural gradient descent (NGD) [1], which involves preconditioning a gradient with the inverse Fisher information matrix (FIM) of a distribution, is an effective method for optimising parameters of probability distributions. It would therefore seem desirable to apply NGD to the inner optimisation, yet doing so is not straightforward. While the FIM can be naturally extended to the product of statistical manifolds that form the solution space, computing and inverting it will not generally be tractable, making (the natural extension of) NGD in this space infeasible.

Consider instead  $\tilde{p}_i^{(t)} \in \mathcal{F}$  with natural parameter  $\eta_i^{(t)}(\lambda_i) = \theta_0 + \sum_j \lambda_j^{(t)} + \alpha^{-1}(\lambda_i - \lambda_i^{(t)})$ . The  $t$  superscript on the site parameters indicates that they are fixed for the current iteration, and so the distribution is fully parameterised by  $\lambda_i$ . Note that when  $\lambda_j = \lambda_j^{(t)} \forall j$ , we have  $\tilde{p}_i^{(t)} = p$ . Proposition 1, which we prove in Appendix C, states that the moment-matching updates of EP can be viewed as performing NGD in  $L$  with respect to *mean parameters* of  $\tilde{p}_i^{(t)}$ .

We will make use of the following properties: for an exponential family with log partition function  $A(\cdot)$ , the gradient  $\nabla A(\cdot)$  provides the map from natural to mean parameters, and this mapping is one-to-one for minimal families, with the inverse given by  $\nabla A^*(\cdot)$ . See Appendix A for details.

**Proposition 1.** *For  $\alpha > 0$ , the moment-matching update of EP (4) is equivalent to performing an NGD step in  $L$  with respect to the mean parameters of  $\tilde{p}_i^{(t)}$  with step size  $\alpha^{-1}$ . That is, for  $\mu_i = \mathbb{E}_{\tilde{p}_i^{(t)}(z)}[s(z)]$ , and  $\tilde{F}_i^{(t)}(\mu_i)$  the FIM of  $\tilde{p}_i^{(t)}$  with respect to  $\mu_i$ , we have*

$$\mu_i - \alpha^{-1} \left[ \tilde{F}_i^{(t)}(\mu_i) \right]^{-1} \frac{\partial L}{\partial \mu_i} = \left( \nabla A \circ \eta_i^{(t)} \right) \left( \lambda_i - \alpha \left( \theta_0 + \sum_j \lambda_j - \nabla A^*(\mathbb{E}_{p_i(z)}[s(z)]) \right) \right). \quad (7)$$

Note that the right hand side of (7) just maps update (4) to mean parameters of  $\tilde{p}_i^{(t)}$ .<sup>4</sup> We discussed in Section 2 that noise in the moment estimates results in bias in the update to  $\lambda_i$  of EP, due to the noise being passed through the nonlinear map  $\nabla A^*(\cdot)$ . This alone would not be a problem if the updates followed unbiased descent direction estimates in some other fixed parameterisation. Let  $\eta_i = \nabla A^*(\mu_i)$ ; then, from the definition of  $L$  and  $\mu_i$ , we have

$$\frac{\partial L}{\partial \mu_i} = \frac{\partial \eta_i}{\partial \mu_i} \frac{\partial \lambda_i}{\partial \eta_i} \left( \nabla A(\theta_0 + \sum_j \lambda_j) - \mathbb{E}_{p_i(z)}[s(z)] \right), \quad (8)$$

and so when  $\mathbb{E}_{p_i(z)}[s(z)]$  is estimated with unbiased samples, the NGD update (7) in  $\mu_i$  is also unbiased. However, a *sequence* of updates introduces bias. This is because the parameterisation changes from one update to the next, with the mean parameters of  $\tilde{p}_i^{(t)}$  mapped to those of  $\tilde{p}_i^{(t+1)}$  by

$$\mu_i^{(t+1)} = \left( \nabla A \circ \eta_i^{(t+1)} \circ (\eta_i^{(t)})^{-1} \circ \nabla A^* \right) (\mu_i^{(t)}), \quad (9)$$

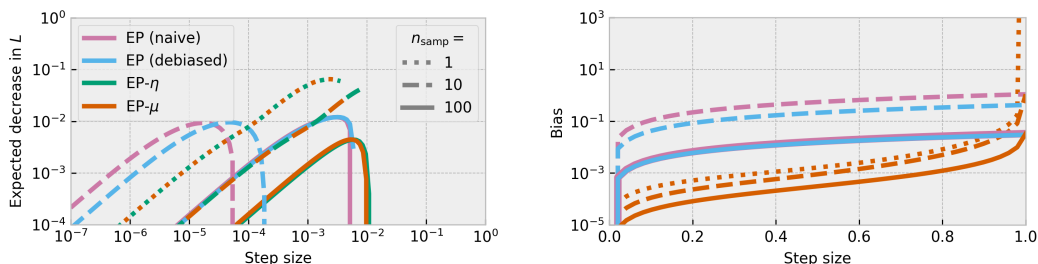
where  $(\eta_i^{(t)})^{-1}(\cdot)$  is the inverse of  $\eta_i^{(t)}(\cdot)$ , and  $\eta_i^{(t+1)}(\cdot)$  is defined using the site parameters *after* the update at time  $t$ . This map is not linear in general, and so an unbiased, noisy update of  $\mu_i$  at one time step, results in bias when mapped to the next. This bias makes the EP updates unstable in the presence of MC noise. This has led previous work to use methods, specific to  $\mathcal{F}$ , for obtaining approximately unbiased *natural* parameter estimates from samples. However, even with these debiasing methods, a relatively large number of samples is still needed in practice [44, 47].

We now use the natural gradient interpretation of the EP updates to motivate two new variants that are far more robust to MC noise; in particular, they are stable, and most sample-efficient, when updates are estimated with just a single sample. Furthermore, unlike methods that rely on debiasing estimators, they do not require sample thinning (see Section 3.4). This largely eliminates two hyperparameters for the practitioner. While practical considerations, such as ensuring efficient use of parallel hardware, may justify using more than one sample per update, this can in principle be tuned *a priori*, much like the batch size hyperparameter of stochastic gradient descent.

### 3.2 EP- $\eta$

We showed in the previous section that bias is introduced into the sequence of NGD updates due to a nonlinear map from one parameterisation to the next. If the map were linear, the sequence

<sup>4</sup>Note the apparent contradiction that by decreasing  $\alpha$  (increasing the damping) we actually *increase* the NGD step size. This is resolved by observing that the definition of  $\tilde{p}_i^{(t)}$  also changes with  $\alpha$ .



(a) Expected decrease in  $L$  after  $100/n_{\text{samp}}$  steps. Performing e.g.  $100 \times 1$ -sample steps, or  $10 \times 10$ -sample steps, achieves a much larger decrease in  $L$  than a single 100-sample step. (b) Magnitude of the bias in  $\lambda_i$  after a single parallel update, averaged over all sites and dimensions. The bias of EP- $\mu$  shrinks far faster as the step size decreases than that of EP. EP- $\eta$  is always unbiased.

Figure 1: The effect of step size ( $\alpha$  or  $\epsilon$ ) and number of samples ( $n_{\text{samp}}$ ) on different EP variants, in the clutter problem of Minka [33]. EP (naive) uses maximum likelihood estimation for the updates, and EP (debiased) uses the estimator of Xu et al. [47]. Step size corresponds to  $\alpha$  for EP, and  $\epsilon$  for EP- $\mu$  and EP- $\eta$ . 1-sample updates are not possible for EP, hence those traces are not visible.

would remain unbiased. This can be achieved by performing NGD with respect to  $\eta_i$ , the *natural* parameters of  $\tilde{p}_i^{(t)}$ ; then, the map from one parameterisation to the next (by equating  $\lambda_i$ ) is given by  $\eta_i^{(t+1)} \circ (\eta_i^{(t)})^{-1}$ , which is linear. The NGD direction in  $L$  with respect to  $\tilde{p}_i^{(t)}$  and  $\eta_i$  is given by

$$-\left[\tilde{F}_i(\eta_i)\right]^{-1} \frac{\partial L}{\partial \eta_i} = -\alpha \frac{\partial \eta_i}{\partial \mu_i}^\top \left( \nabla A(\theta_0 + \sum_j \lambda_j) - \mathbb{E}_{p_i(z)}[s(z)] \right); \quad (10)$$

see Appendix D for a derivation. Note that  $\alpha$  plays a similar role as the NGD step size in this parameterisation, but we fix  $\alpha = 1$  here, and introduce an explicit NGD step size  $\epsilon$ . The resulting update can be expressed directly as an update in  $\lambda_i$ , by applying  $(\eta_i^{(t)})^{-1}$  to the updated  $\eta_i$ , giving

$$\lambda_i \leftarrow \lambda_i - \epsilon \frac{\partial \eta_i}{\partial \mu_i}^\top \left( \nabla A(\theta_0 + \sum_j \lambda_j) - \mathbb{E}_{p_i(z)}[s(z)] \right). \quad (11)$$

We can use automatic differentiation to efficiently compute (11), by recognising the second term as a Jacobian-vector product (JVP) with respect to  $\eta_i(\mu_i) = \nabla A^*(\mu_i)$ .<sup>5</sup> We call the resulting procedure—which is given in Algorithm 2—EP- $\eta$ , to emphasise that we have simply changed to a *natural* parameterisation for the NGD update of EP. The unbiased updates of EP- $\eta$  allow it to be more sample-efficient than EP by using a small number of samples per iteration. This is demonstrated using a stochastic version of the clutter problem of Minka [33] in Figure 1a.

### 3.3 EP- $\mu$

The bias introduced by the updates of EP cannot be mitigated by reducing  $\alpha$  (increasing the damping) without also proportionally sacrificing the amount of progress made by each update. More concretely, let the bias in dimension  $d$  of  $\mu_i^{(t+1)}$ , after an update at time  $t$ , be defined as  $E[\mu_i^{(t+1)} - \bar{\mu}_i^{(t+1)}]_d$ , where  $\bar{\mu}_i^{(t+1)}$  is the value of  $\mu_i^{(t+1)}$  after a noise-free update, and expectation is taken over the sampling distributions of all parallel updates at time  $t$ ; then, Proposition 2 below, which we prove in Appendix F, summarises the effect of decreasing  $\alpha$  on EP.

**Proposition 2.** *After update (4) is executed in parallel over  $i$ , as  $\alpha \rightarrow 0^+$ , both the expected decrease in  $L$ , and the bias  $E[\mu_i^{(t+1)} - \bar{\mu}_i^{(t+1)}]_d$ , are  $O(\alpha)$  for all  $d$ .*

Proposition 1 at the beginning of this section states that update (4) can be viewed as performing an NGD step with respect to  $\mu_i$  with a step size of  $\alpha^{-1}$ . However, changing  $\alpha$  also has the effect of changing the definition of  $\tilde{p}_i^{(t)}$ . It is then natural to wonder what happens if we fix  $\alpha = 1$  and

<sup>5</sup>This can be computed using either forward *or* reverse mode automatic differentiation, as  $\frac{\partial \eta_i}{\partial \mu_i}$  is symmetric.

introduce an explicit step size  $\epsilon$  for NGD, resulting in the update

$$\mu_i \leftarrow \mu_i - \epsilon \left( \nabla A(\theta_0 + \sum_j \lambda_j) - \mathbb{E}_{p_i(z)}[s(z)] \right); \quad (12)$$

see Appendix E for a derivation. It turns out that in doing so, when we decrease  $\epsilon$ , the bias shrinks far faster than the expected decrease in  $L$ .

**Proposition 3.** *After update (12) is executed in parallel over  $i$ , as  $\epsilon \rightarrow 0^+$ , the expected decrease in  $L$  is  $O(\epsilon)$ , and the bias  $E[\mu_i^{(t+1)} - \bar{\mu}_i^{(t+1)}]_d$  is  $O(\epsilon^2)$ , for all  $d$ .*

Proposition 3, which we prove in Appendix F, tells us that by using update (12), we can reduce the bias to arbitrarily small levels while still making progress in decreasing  $L$ . Update (12) can also be expressed directly as an update in  $\lambda_i$  by applying  $(\eta^{(t)})^{-1} \circ \nabla A^*$ , giving

$$\lambda_i \leftarrow \nabla A^* \left( (1 - \epsilon) \nabla A(\theta_0 + \sum_j \lambda_j) + \epsilon \mathbb{E}_{p_i(z)}[s(z)] \right) - \theta_0 - \sum_{j \neq i} \lambda_j, \quad (13)$$

which has the simple interpretation of performing EP, but with damping of the moments instead of the site parameters. We call this variant EP- $\mu$ , again to indicate that we are simply performing the NGD update of EP in the mean parameter space.<sup>6</sup> The resulting procedure is also given by Algorithm 2.

---

**Algorithm 2** EP- $\eta$  and EP- $\mu$  (differences with Algorithm 1 are highlighted in green)

---

**Require:**  $\mathcal{F}$ ,  $\theta_0$ ,  $\{\beta_i\}_i$ ,  $\{\ell_i(z)\}_i$ ,  $\{\lambda_i\}_i$ ,  $n_{\text{inner}}$ ,  $\epsilon$   
**while** not converged **do**  
     $\theta_i \leftarrow \theta_0 + \sum_j \lambda_j$  for  $i = 1$  to  $m$   
    **for** 1 to  $n_{\text{inner}}$  **do**  
        **for**  $i = 1$  to  $m$  *in parallel* **do**  
            update  $\lambda_i$  using (11) for EP- $\eta$ , or (13) for EP- $\mu$   
**return**  $\{\lambda_i\}_i$

---

The computational cost of EP- $\mu$  is lower than that of EP- $\eta$  because it does not require JVPs through  $\nabla A^*(\cdot)$ .<sup>7</sup> The drawback is that the updates of EP- $\mu$  do still retain some bias; however, we find that the bias of EP- $\mu$  typically has negligible impact on its performance relative to EP- $\eta$ . This is evident in the clutter problem of Minka [33], as shown in Figure 1a, as well as in the larger scale experiments of Section 4. Figure 1b illustrates how quickly the bias in  $\lambda_i$  shrinks as the step size of EP- $\mu$  is decreased; note that the results of this subsection are stated in terms of  $\mu_i$ , but it is straightforward to show that equivalent results also hold for  $\lambda_i$  using Taylor series arguments.

### 3.4 Related work

EP was combined with MC moment estimates by Xu et al. [47] in a method called *sampling via moment sharing* (SMS), and later by Vehtari et al. [44] in the context of hierarchical models. In both works, when  $\mathcal{F}$  was multivariate normal—arguably the most useful case—the authors used an estimator for the updates that is unbiased when  $\tilde{p}_i$  is also multivariate normal. Although this estimator is only *approximately* unbiased in general, it can help to stabilise the updates significantly. Even so, it is necessary to use a relatively large number of samples for the updates, with several hundred or more being typical. Using many samples per update is inefficient, as the update direction can change from one iteration to the next. Furthermore, such estimators typically rely on a known number of *independent* samples; samples drawn using Markov chain Monte Carlo (MCMC) methods are generally autocorrelated, necessitating the use of sample thinning before the estimators can be applied. This adds another hyperparameter to the procedure—the thinning ratio—and it is also inefficient due to the discarding of samples. The practitioner is required to choose the number of samples, the thinning ratio, and the amount of damping, all of which affect the accuracy, stability, and computational efficiency of the procedure. There is no easy way to choose these *a priori*, forcing the practitioner to either set them conservatively (favouring accuracy and stability), or to find appropriate settings by trial and error, both of which are likely to expend time and computation unnecessarily.

<sup>6</sup>EP too is performing NGD in mean parameters, but using a step size that also affects the distribution  $\tilde{p}_i$ .

<sup>7</sup>See Appendix G for a detailed discussion of the computational costs of EP- $\eta$  and EP- $\mu$ .

The stochastic natural gradient EP (SNEP) method of Hasenclever et al. [14] optimises the same variational objective as EP, but performs stochastic natural gradient descent with respect to a mean parameterisation (under  $\mathcal{F}$ ) of the site potentials in order to perform the inner minimisation. Its natural gradient updates are unbiased in the presence of MC noise, allowing them to be performed with as little as one sample, without relying on  $\mathcal{F}$ -specific debiasing estimators, or the sample thinning that would entail. The authors found that in some settings, accurate point estimates can be obtained fairly rapidly with SNEP. However, we find that SNEP typically converges far slower than EP, consistent with findings in Vehtari et al. [44]. In SNEP the site potentials are treated as bona fide distributions for the purposes of optimisation, and can be seen as playing the role of surrogate distributions for NGD [42]. The results of this section showed that EP, EP- $\eta$  and EP- $\mu$  are closely related to SNEP; they too can be viewed as performing NGD of  $L$  with respect to surrogate distributions ( $\tilde{p}_i$ ), but with distributions that are more closely matched with those being optimised. This allows them to retain the same benefits as SNEP, but with faster convergence.

We note that Xu et al. [47] and Hasenclever et al. [14] also proposed methods for performing updates in an asynchronous fashion, significantly reducing the frequency and cost of communication between nodes in distributed settings. In principle, these methods could be combined with those presented in this paper, but we do not consider them further here.

## 4 Evaluation

In this section we demonstrate the efficacy of EP- $\eta$  and EP- $\mu$  on a variety of probabilistic inference tasks. In each experiment, the task was to perform approximate Bayesian inference of unobserved parameters  $z$ , given some observed data  $\mathcal{D}$ . All of the models in these experiments followed the same general structure, consisting of a minimal exponential family prior over  $z$ , and a partition of the data  $\{\mathcal{D}_i\}_{i=1}^m$ , where each block  $\mathcal{D}_i$  depends on both  $z$  and an additional vector of *local* latent variables  $w_i$  that also depend on  $z$ ; that is, the joint density has structure

$$p_0(z) \prod_{i=1}^m p(w_i | z) p(\mathcal{D}_i | w_i), \quad (14)$$

where  $p_0 \in \mathcal{F}$ . This is shown graphically in Appendix H. To perform approximate inference of  $z$ , we first define  $\ell_i(z)$  as the log likelihood of  $\mathcal{D}_i$  given  $z$ , with  $w_i$  marginalised out; that is,

$$\ell_i(z) = \log \int p(\mathcal{D}_i, w_i | z) dw_i. \quad (15)$$

Then, given  $p_0(z)$  and  $\{\ell_i(z)\}_i$ , we define  $p^*(z)$  as (1), and proceed to find an approximation  $p(z) \approx p^*(z)$  using the methods described in earlier sections. Note that sampling from the tilted distribution  $p_i(z)$  requires jointly sampling over  $z$  and  $w_i$  and taking the marginal. EP is a particularly appealing framework for performing inference in this setting, as the dimensionality of the sampled distributions is constant with respect to  $m$ , mitigating the curse of dimensionality experienced by conventional MCMC approaches [44]. In our experiments we used NUTS [24] to perform the sampling, consistent with prior work [44, 47]. In each experiment we compared EP- $\eta$  and EP- $\mu$  with EP, in the manner used by Xu et al. [47], Vehtari et al. [44]. Where  $\mathcal{F}$  was MVN, we also compared to SNEP [14]. For the models with NIW  $\mathcal{F}$ , we were unable to find an initialisation for SNEP that would allow us to perform a meaningful comparison; we discuss this more in Appendix H.

To evaluate the performance of the different variants, we monitored KL divergence to an estimate of the optimum, obtained by running EP with a large number of samples. We used 500 different hyperparameter settings for each variant, chosen using random search, and repeated each run 5 times using different random seeds for NUTS. All runs of EP- $\eta$  and EP- $\mu$  were performed with  $n_{\text{samp}} = 1$  and  $n_{\text{inner}} = 1$ . The results of these experiments are summarised in Figure 2

We see that EP- $\eta$  and EP- $\mu$  can typically reach a given level of accuracy (distance from optimum) faster than EP, often significantly so. We stress that the frontiers for EP- $\eta$  and EP- $\mu$  are traced out with  $n_{\text{samp}}$  and  $n_{\text{inner}}$  each fixed to 1, with no sample thinning, varying only the step size hyperparameter  $\epsilon$ , with higher accuracy/cost regions of the frontier corresponding to lower values of  $\epsilon$ . In contrast, to trace out the frontier of EP we must jointly vary  $\alpha$ ,  $n_{\text{samp}}$ , and the thinning ratio; see Appendix I for examples of this effect. The performances of EP- $\eta$  and EP- $\mu$  are very similar. We found SNEP to be significantly slower than the other methods, consistent with findings by Vehtari et al. [44]. Pareto frontiers with respect to wall-clock time can be found in Appendix J. We now provide a brief overview of individual experiments, with further details given in Appendix H.

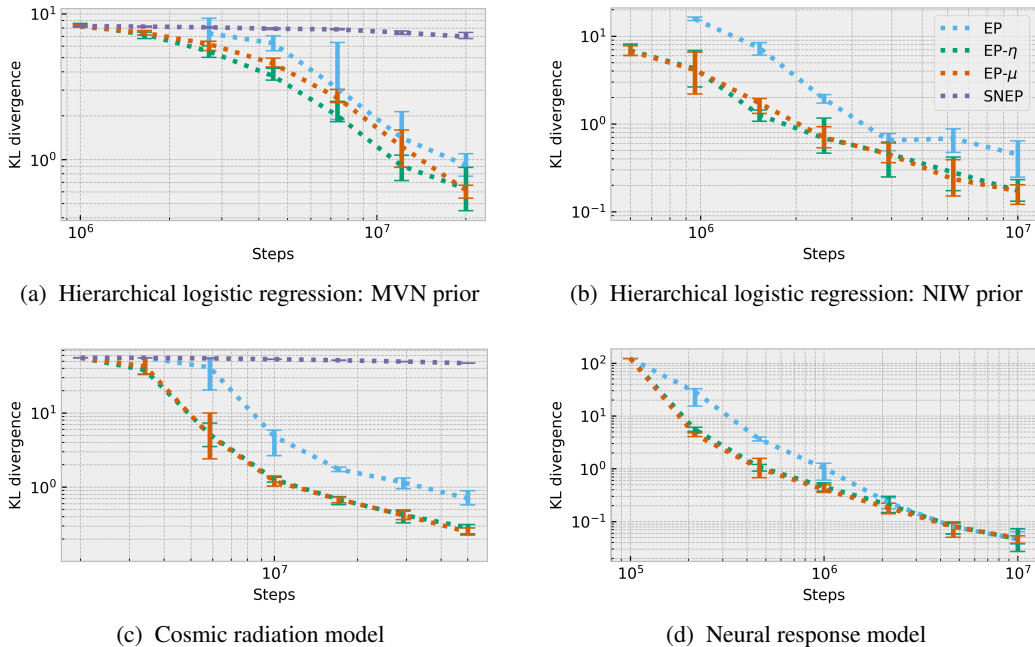


Figure 2: Pareto frontier showing the number of NUTS steps ( $x$ -axis) against the KL divergence from  $p$  to an estimate of the optimum ( $y$ -axis). Each point on the plot marks the lowest average KL divergence attained by *any* hyperparameter setting by that step count. Error bars mark the full range of values for the marked hyperparameter setting across 5 random seeds.

#### 4.1 Hierarchical logistic regression

Hierarchical logistic regression is used to perform binary classification in a number of groups when the extent to which data should be pooled across groups is unknown [12]. Each of the  $m$  groups has its own covariates and binary response variables, collectively denoted by  $\mathcal{D}_i$ , as well as regression coefficients  $w_i$ . The groups are related through prior parameters  $z$ , which parameterise the group-level coefficient prior densities  $p(w_i | z)$ . We performed two experiments in this setting.

**Synthetic data with MVN prior** In this experiment, the group-level prior density  $p(w_i | z)$  was a product of independent normal densities, with  $p_0 \in \mathcal{F}$  being a multivariate normal (MVN) prior over the means and log-variances. We used the same synthetic data generation as Vehtari et al. [44], which was designed to be challenging for EP. In this experiment  $z \in \mathbb{R}^8$ ,  $w_i \in \mathbb{R}^4 \forall i$ ,  $m = 16$ , and each of the  $m$  regression tasks had  $n = 20$  observations. Results are shown in Figure 2a.

**Political survey data with NIW prior** In this experiment, each of  $m = 50$  nested regression tasks corresponded to political survey responses from a particular US state, with 7 predictor variables corresponding to characteristics of a given survey respondent, so that  $w_i \in \mathbb{R}^7$  for  $i = 1, \dots, m$ . The state-level prior density  $p(w_i | z)$  was that of a MVN distribution, with  $p_0 \in \mathcal{F}$  being a normal-inverse-Wishart (NIW) prior on the mean and covariance matrix. This structure allows for correlation of regression coefficients across states. The data, taken from the 2018 Cooperative Congressional Election Study, related to support for allowing employers to decline coverage of abortions in insurance plans [29, 39]. We truncated the data slightly so that each state contained  $n = 97$  survey responses. Results are shown in Figure 2b.

#### 4.2 Cosmic radiation model

A hierarchical Bayesian model was used by Vehtari et al. [44] to capture the nonlinear relationship between diffuse galactic far ultraviolet radiation and 100- $\mu\text{m}$  infrared emission in various sectors of the observable universe, using data obtained from the Galaxy Evolution Explorer telescope. In

this model each  $w_i \in \mathbb{R}^9$  parameterised a nonlinear regression model using data obtained from one of  $m$  sections of the observable universe. The  $m$  regression problems were related through hyperparameters  $z \in \mathbb{R}^{18}$ , which parameterised the section-level coefficient prior densities  $p(w_i | z)$  for  $i = 1, \dots, m$ .  $p_0 \in \mathcal{F}$  was MVN. The specifics of the nonlinear regression model are quite involved and we refer the reader to Vehtari et al. [44] for details.

Vehtari et al. [44] used EP to perform inference in this model. We were unable to obtain the dataset, and so we generated synthetic data using hyperparameters parameters that were tuned by hand to try and match the qualitative properties of the original data; see Appendix K for examples. We used a reduced number of  $m = 36$  sites and  $n = 200$  observations per site to allow us to perform a comprehensive hyperparameter search. Results are shown in Figure 2c.

### 4.3 Neural response model

A common task in neuroscience is to model the firing rates of neurons under various conditions. We performed inference in a hierarchical Bayesian neural response model, using recordings of V1 complex cells in an anaesthetised adult cat [3]. In this dataset, 10 neurons in a specific area of cat V1 were simultaneously recorded under the presentation of 18 different visual stimuli, each repeated 8 times, for a total of 144 trials. We modelled the observed spike counts of the 10 neurons in each trial as Poisson, with latent (log) intensities being MVN, with mean and covariance (collectively  $z \in \mathbb{R}^{65}$ ) drawn from a NIW prior  $p_0 \in \mathcal{F}$ . Inference of  $z$  amounted to inferring the means, and inter-neuron correlations, of latent log firing rates across stimuli. We grouped the data into  $m = 8$  batches of  $n = 18$  trials each, so that the latent log firing rates for all trials in batch  $i$  were jointly captured by  $w_i \in \mathbb{R}^{180}$ . Results are shown in Figure 2d.

## 5 Conclusion

In this work, we used a novel interpretation of the moment-matching updates of EP to motivate two new EP variants that are far more robust to MC noise. We demonstrated that these variants can offer an improved speed-accuracy trade-off compared to their predecessors, and are easier to tune.

**Limitations** We largely assumed that the drawing of MC samples is the dominant cost. In practice, other costs become relevant, which may shift the balance in favour of using more samples to estimate updates. We discuss this in Appendix G, along with strategies for reducing computational overheads. We note, however, that wall-clock time results for our experiments (in Appendix J) are in line with the results of Section 4. When EP and its variants—including those introduced here—are combined with MC methods, the underlying samplers typically have hyperparameters of their own, which are often adapted using so-called warmup phases. While EP- $\eta$  and EP- $\mu$  significantly reduce the complexity of tuning hyperparameters specific to EP, they do not help with those of the underlying samplers; this means that the complexity of hyperparameter tuning is still greater than that of direct MC methods. We used comprehensive hyperparameter searches in our experiments in order to perform a meaningful comparison with baseline methods, necessarily limiting the scale of problems we could tackle.

**Future work** It would be worthwhile considering how our algorithms can be efficiently implemented for modern parallel compute hardware; e.g., practical performance could be improved by using sampling kernels that are themselves designed for efficient parallel execution [23]. Performance may also be improved in distributed settings by using asynchronous extensions to minimise communication overheads [14, 47]. The need to tune sampling hyperparameters could be obviated by using information from  $p$  to set them directly; e.g., when  $p \in \mathcal{F}$  is MVN, its precision matrix could be used directly as the mass matrix hyperparameter in Hamiltonian Monte Carlo schemes. We would also like to apply our methods to large-scale problems. We leave investigation of these ideas to future work.

## References

- [1] S.-i. Amari. Natural Gradient Works Efficiently in Learning. *Neural Computation*, 1998.
- [2] R. Anil, V. Gupta, T. Koren, K. Regan, and Y. Singer. Scalable second order optimization for deep learning. *arXiv:2002.09018*, 2021.

- [3] T. Blanche. Multi-neuron recordings in primary visual cortex., 2009.
- [4] M. Blondel, Q. Berthet, M. Cuturi, R. Frostig, S. Hoyer, F. Llinares-López, F. Pedregosa, and J.-P. Vert. Efficient and modular implicit differentiation. *arXiv:2105.15183*, 2021.
- [5] J. Bradbury, R. Frostig, P. Hawkins, M. J. Johnson, C. Leary, D. Maclaurin, G. Necula, A. Paszke, J. VanderPlas, S. Wanderman-Milne, and Q. Zhang. JAX: composable transformations of Python+NumPy programs, 2018.
- [6] S. Brooks, A. Gelman, G. Jones, and X.-L. Meng. *Handbook of Markov Chain Monte Carlo*. Chapman and Hall/CRC, 2011.
- [7] T. Bui, D. Hernandez-Lobato, J. Hernandez-Lobato, Y. Li, and R. Turner. Deep gaussian processes for regression using approximate expectation propagation. *International Conference on Machine Learning*, 2016.
- [8] T. D. Bui, J. Yan, and R. E. Turner. A unifying framework for gaussian process pseudo-point approximations using power expectation propagation. *Journal of Machine Learning Research*, 2017.
- [9] W. Chu and Z. Ghahramani. Gaussian processes for ordinal regression. *Journal of Machine Learning Research*, 2005.
- [10] J. P. Cunningham, K. V. Shenoy, and M. Sahani. Fast gaussian process methods for point process intensity estimation. *International Conference on Machine Learning*, 2008.
- [11] J. P. Cunningham, P. Hennig, and S. Lacoste-Julien. Gaussian probabilities and expectation propagation. *arXiv:1111.6832*, 2013.
- [12] A. Gelman, J. Carlin, H. Stern, D. Dunson, A. Vehtari, and D. Rubin. *Bayesian Data Analysis, Third Edition*. Chapman and Hall/CRC, 2013.
- [13] J. Gonzalez, M. Osborne, and N. Lawrence. Glasses: Relieving the myopia of bayesian optimisation. *International Conference on Artificial Intelligence and Statistics*, 2016.
- [14] L. Hasenclever, S. Webb, T. Lienart, S. Vollmer, B. Lakshminarayanan, C. Blundell, and Y. W. Teh. Distributed bayesian learning with stochastic natural gradient expectation propagation and the posterior server. *Journal of Machine Learning Research*, 2017.
- [15] P. Hennig. Expectation propagation on the maximum of correlated normal variables. Technical report, University of Cambridge, 2009.
- [16] P. Hennig and C. J. Schuler. Entropy search for information-efficient global optimization. *Journal of Machine Learning Research*, 2012.
- [17] P. Hennig, D. Stern, and T. Graepel. Coherent inference on optimal play in game trees. *International Conference on Artificial Intelligence and Statistics*, 2010.
- [18] R. Herbrich, T. Minka, and T. Graepel. Trueskill™: A bayesian skill rating system. *Advances in Neural Information Processing Systems*, 2006.
- [19] D. Hernandez-Lobato and J. M. Hernandez-Lobato. Scalable gaussian process classification via expectation propagation. *International Conference on Artificial Intelligence and Statistics*, 2016.
- [20] J. M. Hernández-Lobato and R. P. Adams. Probabilistic backpropagation for scalable learning of bayesian neural networks. *International Conference on Machine Learning*, 2015.
- [21] T. Heskes and O. Zoeter. Expectation propagation for approximate inference in dynamic bayesian networks. *Uncertainty in Artificial Intelligence*, 2002.
- [22] T. Heskes and O. Zoeter. Extended version of “expectation propagation for approximate inference in dynamic bayesian networks. Technical report, University of Nijmegen, 2003.

- [23] M. Hoffman, A. Radul, and P. Sountsov. An adaptive-mcmc scheme for setting trajectory lengths in hamiltonian monte carlo. *International Conference on Artificial Intelligence and Statistics*, 2021.
- [24] M. D. Hoffman and A. Gelman. The no-u-turn sampler: Adaptively setting path lengths in hamiltonian monte carlo. *Journal of Machine Learning Research*, 2014.
- [25] P. A. d. F. R. Højen-Sørensen, O. Winther, and L. K. Hansen. Mean-field approaches to independent component analysis. *Neural Computation*, 2002.
- [26] W. Jitkrittum, A. Gretton, N. M. O. Heess, S. M. A. Eslami, B. Lakshminarayanan, D. Sejdinovic, and Z. Szabó. Kernel-based just-in-time learning for passing expectation propagation messages. *Uncertainty in Artificial Intelligence*, 2015.
- [27] P. Jylänki, J. Vanhatalo, and A. Vehtari. Robust gaussian process regression with a student- $t$  likelihood. *Journal of Machine Learning Research*, 2011.
- [28] Y. Li, J. M. Hernández-Lobato, and R. E. Turner. Stochastic expectation propagation. *Advances in Neural Information Processing Systems*, 2015.
- [29] J. Lopez-Martin, J. Phillips, and A. Gelman. Multilevel regression and poststratification case studies, 2022.
- [30] T. Minka. Power ep. Technical report, Microsoft, 2004.
- [31] T. Minka and J. Lafferty. Expectation-propagation for the generative aspect model. *Uncertainty in Artificial Intelligence*, 2002.
- [32] T. Minka, R. Cleven, and Y. Zaykov. Trueskill 2: An improved bayesian skill rating system. Technical report, Microsoft, 2018.
- [33] T. P. Minka. *A family of algorithms for approximate Bayesian inference*. PhD thesis, Massachusetts Institute of Technology, 2001.
- [34] A. Naish-guzman and S. Holden. The generalized fitc approximation. *Advances in Neural Information Processing Systems*, 2007.
- [35] U. Nodelman, D. Koller, and C. Shelton. Expectation propagation for continuous time bayesian networks. *Uncertainty in Artificial Intelligence*, 2005.
- [36] M. Opper and O. Winther. Gaussian processes for classification: Mean-field algorithms. *Neural Computation*, 2000.
- [37] M. Opper, U. Paquet, and O. Winther. Improving on expectation propagation. *Advances in Neural Information Processing Systems*, 2008.
- [38] D. Phan, N. Pradhan, and M. Jankowiak. Composable effects for flexible and accelerated probabilistic programming in numpyro, 2019.
- [39] B. Schaffner, S. Ansolabehere, and S. Luks. CCES common content 2018, 2019.
- [40] M. Seeger and H. Nickisch. Fast convergent algorithms for expectation propagation approximate bayesian inference. *International Conference on Artificial Intelligence and Statistics*, 2011.
- [41] J. So. Estimating the normal-inverse-wishart distribution. *arXiv:2405.16088*, 2024.
- [42] J. So and R. E. Turner. Optimising distributions with natural gradient surrogates. *International Conference on Artificial Intelligence and Statistics*, 2024.
- [43] R. E. Turner and M. Sahani. Probabilistic amplitude and frequency demodulation. *Advances in Neural Information Processing Systems*, 2011.
- [44] A. Vehtari, A. Gelman, T. Sivula, P. Jylänki, D. Tran, S. Sahai, P. Blomstedt, J. P. Cunningham, D. Schiminovich, and C. P. Robert. Expectation propagation as a way of life: A framework for bayesian inference on partitioned data. *Journal of Machine Learning Research*, 2020.

- [45] M. Wainwright and M. Jordan. Graphical models, exponential families, and variational inference. *Foundations and Trends in Machine Learning*, 2008.
- [46] M. Welling and J. J. Lim. A distributed message passing algorithm for sensor localization. *International Conference on Artificial Neural Networks*, 2007.
- [47] M. Xu, B. Lakshminarayanan, Y. W. Teh, J. Zhu, and B. Zhang. Distributed bayesian posterior sampling via moment sharing. *Advances in Neural Information Processing Systems*, 2014.
- [48] O. Zoeter and T. Heskes. Gaussian quadrature based expectation propagation. *Proceedings of the Tenth International Workshop on Artificial Intelligence and Statistics*, 2005.

## A Exponential families of distributions

In this appendix, we give a very brief overview of exponential families of distributions. This is a highly condensed summary of relevant material from Wainwright and Jordan [45], and we refer the reader to the original work for a far more detailed treatment.

The exponential family of distributions  $\mathcal{F}$ , defined by the ( $d$ -dimensional, vector-valued) sufficient statistic function  $s(\cdot)$  and base measure  $\nu(\cdot)$ , has density function

$$p(z) = \exp(\theta^\top s(z) - A(\theta)), \quad (16)$$

taken with respect to  $\nu(\cdot)$ , where  $A(\theta) = \log \int \exp(\theta^\top s(z)) d\nu(z)$  is known as the *log partition function*.  $\theta \in \Omega$  are known as the *natural parameters*, and are used to index a specific member of  $\mathcal{F}$ .  $\Omega$  is the set of normalisable natural parameters of  $\mathcal{F}$ , given by

$$\Omega = \left\{ \theta \in \mathbb{R}^d \mid \int \exp(\theta^\top s(z)) d\nu(z) < \infty \right\}, \quad (17)$$

and is known as the *natural domain* of  $\mathcal{F}$ .  $\Omega$  is a convex set, and when it is open, the family  $\mathcal{F}$  is said to be *regular*; we shall only consider regular families in this work. When the components of  $s(\cdot)$  are linearly independent,  $\mathcal{F}$  is said to be *minimal*. For minimal families, each distribution in the family is associated with a unique natural parameter vector  $\theta$ . An exponential family that is not minimal is said to be *overcomplete*, in which case, each distribution is associated with an entire affine subspace of  $\Omega$ .

The expected sufficient statistics of a distribution with density  $p(\cdot)$  with respect to base measure  $\nu(\cdot)$ , are given by  $\mathbb{E}_{p(z)}[s(z)]$ . The *mean domain*,  $\mathcal{M}$ , is defined as the set of expected sufficient statistics that can be attained by *any* density  $p(\cdot)$  with respect to base measure  $\nu(\cdot)$ ; that is,

$$\mathcal{M} = \left\{ \mu \in \mathbb{R}^d \mid \exists p(\cdot) : \int p(z) s(z) d\nu(z) = \mu \right\}. \quad (18)$$

All vectors in the interior of  $\mathcal{M}$ ,  $\mathcal{M}^\circ$ , are realisable by a member of  $\mathcal{F}$ , and so  $\mu \in \mathcal{M}^\circ$  provides an alternative parameterisation of  $\mathcal{F}$ , in which  $\mu$  are known as the *mean parameters*.

For minimal families,  $A(\cdot)$  is strictly convex on  $\Omega$ . The convex dual of  $A(\cdot)$  is defined as

$$A^*(\mu) = \max_{\theta \in \Theta} \theta^\top \mu - A(\theta), \quad (19)$$

and on  $\mathcal{M}^\circ$ ,  $A^*(\mu)$  is equal to the negative entropy of the member of  $\mathcal{F}$  with mean parameter  $\mu$ , hence  $A^*(\cdot)$  is also referred to as the *negative entropy function*.

The mean parameters of the member of  $\mathcal{F}$  with natural parameter  $\theta$  can be obtained by  $\mu = \nabla A(\theta)$ . For minimal families, this mapping is one-to-one, and the reverse map is given by  $\theta = \nabla A^*(\mu)$ . For this reason,  $\nabla A(\cdot)$  and  $\nabla A^*(\cdot)$  are sometimes referred to as the *forward mapping* and *backward mapping* respectively. In this work, we say that a family  $\mathcal{F}$  is *tractable* if both the forward and backward mappings can be evaluated efficiently.

The Fisher information matrix (FIM) of an exponential family distribution, with respect to natural parameters  $\theta$ , is given by,  $F(\theta) = \nabla^2 A(\theta)$ . Furthermore, in minimal families, the FIM with respect

to mean parameters  $\mu$  is given by  $F(\mu) = \nabla^2 A^*(\mu)$ . Using the forward and backward mappings, we also have

$$F(\theta) = \frac{\partial \mu}{\partial \theta} \quad (20)$$

$$F(\mu) = \frac{\partial \theta}{\partial \mu}, \quad (21)$$

and from the inverse function theorem,

$$F(\theta)^{-1} = \frac{\partial \theta}{\partial \mu} \quad (22)$$

$$F(\mu)^{-1} = \frac{\partial \mu}{\partial \theta}. \quad (23)$$

## B EP inner update derivation

Begin by taking gradients of (3), with respect to  $\lambda_i$ , giving

$$\nabla_{\lambda_i} L(\eta_1, \dots, \eta_m, \lambda_1, \dots, \lambda_m) = \nabla A \left( \eta_0 + \sum_j \lambda_j \right) - \nabla_{\lambda_i} A_i((\eta_i - \beta_i^{-1} \lambda_i, \beta_i^{-1})). \quad (24)$$

At a minimum of  $L$  with respect to  $\lambda_i$ , both sides of (24) must be equal to zero. We can use this to define a fixed-point condition with respect to  $\lambda_i$ , and its updated value  $\lambda'_i$

$$\begin{aligned} \nabla A \left( \eta_0 + \lambda'_i + \sum_{j \neq i} \lambda_j \right) &= \nabla_{\lambda_i} A_i((\eta_i - \beta_i^{-1} \lambda_i, \beta_i^{-1})) \\ &= \mathbb{E}_{p_i(z)}[s(z)] \end{aligned} \quad (25)$$

where  $p_i \in \mathcal{F}_i$  denotes the  $i$ -th *tilted distribution*, defined by (6). Applying  $\nabla A^*(\cdot)$ , the inverse of  $\nabla A(\cdot)$ , to both sides of (25), and rearranging terms, we recover the moment-matching update of EP

$$\lambda_i \leftarrow \nabla A^* \left( \mathbb{E}_{p_i(z)}[s(z)] \right) - \eta_0 - \sum_{j \neq i} \lambda_j. \quad (26)$$

Often a damping parameter is used to aid convergence, giving the more general update

$$\begin{aligned} \lambda_i &\leftarrow (1 - \alpha) \lambda_i + \alpha \left( \nabla A^* \left( \mathbb{E}_{p_i(z)}[s(z)] \right) - \eta_0 - \sum_{j \neq i} \lambda_j \right) \\ &\leftarrow \lambda_i + \alpha \left( \nabla A^* \left( \mathbb{E}_{p_i(z)}[s(z)] \right) - \eta_0 - \sum_j \lambda_j \right), \end{aligned} \quad (27)$$

where the level of damping is given by  $(1 - \alpha)$ . It was shown by Heskes and Zoeter [22] that (4) follows a decrease direction in  $L$  with respect to  $\lambda_i$ , and so is guaranteed to decrease  $L$  when  $\alpha$  is small enough.

## C Natural gradient view of EP

Let  $\tilde{p}_i^{(t)}$  be the member of  $\mathcal{F}$  with natural parameter  $\eta_i^{(t)}(\lambda_i) = \theta_0 + \sum_j \lambda_j^{(t)} + \alpha^{-1}(\lambda_i - \lambda_i^{(t)})$ . Proposition 1 states that that the moment-matching updates of EP can be viewed as performing NGD in  $L$  with respect to the mean parameters,  $\mu_i$ , of  $\tilde{p}_i^{(t)}$ . We restate the proposition below, and give a proof. Note that the right hand side of (7) maps the EP update (4) onto mean parameters of  $\tilde{p}_i^{(t)}$ . The left hand side of (7) is simply a NGD update in  $\mu_i$ .

**Proposition 1.** *For  $\alpha > 0$ , the moment-matching update of EP (4) is equivalent to performing an NGD step in  $L$  with respect to the mean parameters of  $\tilde{p}_i^{(t)}$  with step size  $\alpha^{-1}$ . That is, for  $\mu_i = \mathbb{E}_{\tilde{p}_i^{(t)}(z)}[s(z)]$ , and  $\tilde{F}_i^{(t)}(\mu_i)$  the FIM of  $\tilde{p}_i^{(t)}$  with respect to  $\mu_i$ , we have*

$$\mu_i - \alpha^{-1} \left[ \tilde{F}_i^{(t)}(\mu_i) \right]^{-1} \frac{\partial L}{\partial \mu_i} = \left( \nabla A \circ \eta_i^{(t)} \right) \left( \lambda_i - \alpha \left( \theta_0 + \sum_j \lambda_j - \nabla A^* \left( \mathbb{E}_{p_i(z)}[s(z)] \right) \right) \right). \quad (7)$$

*Proof.* Taking the left hand side of (7), we have

$$\begin{aligned}
\mu_i - \alpha^{-1} [\tilde{F}_i^{(t)}(\mu_i)]^{-1} \frac{\partial \lambda_i}{\partial \mu_i} &= \mu_i - \alpha^{-1} [\tilde{F}_i^{(t)}(\mu_i)]^{-1} \frac{\partial \lambda_i}{\partial \mu_i} \frac{\partial L}{\partial \lambda_i} \\
&= \mu_i - \alpha^{-1} \left( \frac{\partial \eta_i}{\partial \mu_i} \right)^{-1} \frac{\partial \eta_i}{\partial \mu_i} \frac{\partial \lambda_i}{\partial \eta_i} \frac{\partial L}{\partial \lambda_i} \\
&= \mu_i - \frac{\partial L}{\partial \lambda_i} \\
&= \mu_i - \left( \nabla A(\theta_0 + \sum_j \lambda_j) - \mathbb{E}_{p_i(z)}[s(z)] \right) \\
&= \nabla A(\theta_0 + \sum_j \lambda_j) - \left( \nabla A(\theta_0 + \sum_j \lambda_j) - \mathbb{E}_{p_i(z)}[s(z)] \right) \\
&= \mathbb{E}_{p_i(z)}[s(z)], \tag{28}
\end{aligned}$$

where the penultimate equality follows from the definition  $\mu_i = \mathbb{E}_{\tilde{p}_i^{(t)}(z)}[s(z)]$ , and the fact that  $\lambda_j^{(t)} = \lambda_j \forall j$  before the update. All that remains is to show that the right hand side of (7) is equal to  $\mathbb{E}_{p_i(z)}[s(z)]$ ;

$$\begin{aligned}
&\left( \nabla A \circ \eta_i^{(t)} \right) \left( \lambda_i - \alpha \left( \theta_0 + \sum_j \lambda_j - \nabla A^*(\mathbb{E}_{p_i(z)}[s(z)]) \right) \right) \\
&= \nabla A \left( \alpha^{-1} (\lambda_i - \lambda_i^{(t)}) + \nabla A^*(\mathbb{E}_{p_i(z)}[s(z)]) \right) \\
&= \mathbb{E}_{p_i(z)}[s(z)] \tag{29}
\end{aligned}$$

□

## D EP- $\eta$ update direction derivation

Using the relation  $\eta_i = \eta_i^{(t)}(\lambda_i)$ , and therefore  $\lambda_i = (\eta_i^{(t)})^{-1}(\eta_i)$ , we have

$$\begin{aligned}
- \left[ \tilde{F}_i(\eta_i) \right]^{-1} \frac{\partial L}{\partial \eta_i} &= - \left[ \tilde{F}_i(\eta_i) \right]^{-1} \frac{\partial \lambda_i}{\partial \eta_i} \frac{\partial L}{\partial \lambda_i} \\
&= -\alpha \left( \frac{\partial \mu_i}{\partial \eta_i} \tilde{F}_i(\mu_i) \frac{\partial \mu_i^\top}{\partial \eta_i} \right)^{-1} \frac{\partial L}{\partial \lambda_i} \\
&= -\alpha \left( \frac{\partial \eta_i}{\partial \mu_i}^\top \tilde{F}_i(\mu_i)^{-1} \frac{\partial \eta_i}{\partial \mu_i} \right) \frac{\partial L}{\partial \lambda_i} \\
&= -\alpha \left( \frac{\partial \eta_i}{\partial \mu_i}^\top \frac{\partial \mu_i}{\partial \eta_i} \frac{\partial \eta_i}{\partial \mu_i} \right) \frac{\partial L}{\partial \lambda_i} \\
&= -\alpha \frac{\partial \eta_i}{\partial \mu_i}^\top \left( \nabla A(\theta_0 + \sum_j \lambda_j) - \mathbb{E}_{p_i(z)}[s(z)] \right). \tag{30}
\end{aligned}$$

## E EP- $\mu$ update derivation

For  $\alpha = 1$ , we have

$$\begin{aligned}
\mu_i - \epsilon \left[ \tilde{F}_i(\mu_i) \right]^{-1} \frac{\partial L}{\partial \mu_i} &= \mu_i - \epsilon \left[ \tilde{F}_i(\mu_i) \right]^{-1} \frac{\partial \eta_i}{\partial \mu_i} \frac{\partial \lambda_i}{\partial \eta_i} \frac{\partial L}{\partial \lambda_i} \\
&= \mu_i - \epsilon \left( \frac{\partial \eta_i}{\partial \mu_i} \right)^{-1} \frac{\partial \eta_i}{\partial \mu_i} \frac{\partial \lambda_i}{\partial \eta_i} \left( \nabla A(\theta_0 + \sum_j \lambda_j) - \mathbb{E}_{p_i(z)}[s(z)] \right) \\
&= \mu_i - \epsilon \left( \nabla A(\theta_0 + \sum_j \lambda_j) - \mathbb{E}_{p_i(z)}[s(z)] \right). \tag{31}
\end{aligned}$$

## F Bias of EP and EP- $\mu$

Let the bias in dimension  $d$  of  $\mu_i^{(t+1)}$ , after an update at time  $t$ , be defined as  $E[\mu_i^{(t+1)} - \bar{\mu}_i^{(t+1)}]_d$ , where  $\bar{\mu}_i^{(t+1)}$  is the value of  $\mu_i^{(t+1)}$  after a noise-free update, and expectation is taken over the sampling distributions of all parallel updates at time  $t$ . Propositions 2 and 3, which we restate and prove below, summarise the effect of decreasing  $\alpha$  on EP and EP- $\mu$ .

**Proposition 2.** *After update (4) is executed in parallel over  $i$ , as  $\alpha \rightarrow 0^+$ , both the expected decrease in  $L$ , and the bias  $E[\mu_i^{(t+1)} - \bar{\mu}_i^{(t+1)}]_d$ , are  $O(\alpha)$  for all  $d$ .*

*Proof.* Let  $\eta_i^{(t)}$  and  $\mu_i^{(t)}$  be the pre-update natural and mean parameters of  $\tilde{p}_i(t)$  respectively. Furthermore, let

$$\begin{aligned}\mu_i^{(t)'} &= \mu_i^{(t)} - \alpha^{-1} [\tilde{F}_i^{(t)}]^{-1}(\mu_i) \frac{\partial \lambda_i}{\partial \mu_i} \frac{\partial L}{\partial \lambda_i} + \xi_i \\ &= \mathbb{E}_{p_i(z)}[s(z)] + \xi_i,\end{aligned}\tag{32}$$

be the mean parameters of  $\tilde{p}_i^{(t)}$  after an EP inner update (4) but *before* being mapped to mean parameters of  $\tilde{p}_i^{(t+1)}$  through map (9).  $\xi_i$  is some zero-mean noise, e.g. due to MC variation. The second equality follows from the results of Appendix C. Similarly, let  $\eta_i^{(t)'} = \nabla A^*(\mu_i^{(t)'})$  be the corresponding natural parameters. Now apply map (9) to convert to mean parameters of  $\tilde{p}_i^{(t+1)}$ ,

$$\begin{aligned}\mu_i^{(t+1)} &= \left( \nabla A \circ \eta_i^{(t+1)} \circ (\eta_i^{(t)})^{-1} \circ \nabla A^* \right) (\mu_i^{(t)'}) \\ &= \nabla A \left( \left( \eta_i^{(t+1)} \circ (\eta_i^{(t)})^{-1} \right) \left( \nabla A^* (\mu_i^{(t)'}) \right) \right) \\ &= \nabla A \left( \nabla A^* (\mu_i^{(t)}) + \alpha \sum_j \left( \nabla A^* (\mu_j^{(t)'}) - \nabla A^* (\mu_j^{(t)}) \right) \right),\end{aligned}\tag{33}$$

where the last equality follows from the definition of  $\eta_i^{(t)}(\cdot)$ , and by observing that

$$\begin{aligned}\lambda_j^{(t+1)} - \lambda_j^{(t)} &= \alpha(\eta_j' - \eta_j) \\ &= \alpha \left( A^* (\mu_j^{(t)'}) - \nabla A^* (\mu_j^{(t)}) \right),\end{aligned}\tag{34}$$

for all  $j$ . Let  $\bar{\mu}_i^{(t)'} = \mathbb{E}_{p_i(z)}[s(z)]$  be the mean parameters of  $\tilde{p}_i^{(t)}$  after a *noise-free* update (but before mapping to those of  $\tilde{p}_i^{(t+1)}$ ), so that  $\mu_i^{(t)'} = \bar{\mu}_i^{(t)'} + \xi_i$ . Substituting this in, we have

$$\mu_i^{(t+1)} = \nabla A \left( \nabla A^* (\mu_i^{(t)}) + \alpha \sum_j \left( \nabla A^* (\bar{\mu}_j^{(t)'} + \xi_j) - \nabla A^* (\mu_j^{(t)}) \right) \right).\tag{35}$$

Taking a Taylor expansion around  $\alpha = 0$ , we have

$$\mu_i^{(t+1)} = \mu_i^{(t)} + \alpha \left[ \nabla^2 A \left( \nabla A^* (\mu_i^{(t)}) \right) \right] \left( \sum_j \nabla A^* (\bar{\mu}_j^{(t)'} + \xi_j) - \nabla A^* (\mu_j^{(t)}) \right) + O(\alpha^2).\tag{36}$$

Now subtract the noise-free update  $\bar{\mu}_i^{(t+1)}$ , and take expectations with respect to  $\xi_j$  for  $j = 1, \dots, m$ ,

$$\begin{aligned}\mathbb{E} \left[ \mu_i^{(t+1)} - \bar{\mu}_i^{(t+1)} \right] &= \mathbb{E} \left[ \alpha \left[ \nabla^2 A \left( \nabla A^* (\mu_i^{(t)}) \right) \right] \left( \right. \right. \\ &\quad \left. \left. \sum_j \nabla A^* (\bar{\mu}_j^{(t)'} + \xi_j) - \nabla A^* (\bar{\mu}_j^{(t)'}) \right) + O(\alpha^2) \right].\end{aligned}\tag{37}$$

the first term on the right hand side does not have zero expectation in general— $\nabla A^*(\cdot)$  is not linear—and so the bias is  $O(\alpha)$  as  $\alpha \rightarrow 0^+$ .

To see that the expected change in  $L$  is also  $O(\alpha)$ , take the Taylor expansion of  $L$  along the update direction—obtained by subtracting  $\lambda_i$  from the right hand side of (4)—as a function of the step size around  $\alpha = 0$ ,

$$-\alpha \left( \theta_0 + \sum_{j \neq i} \lambda_j - \nabla A(E_{p_i(z)}[s(z)] + \xi_i) \right)^\top \frac{\partial L}{\partial \lambda_i} + O(\alpha^2), \quad (38)$$

which is clearly  $O(\alpha)$  as  $\alpha \rightarrow^+$ .  $\square$

**Proposition 3.** *After update (12) is executed in parallel over  $i$ , as  $\epsilon \rightarrow 0^+$ , the expected decrease in  $L$  is  $O(\epsilon)$ , and the bias  $E[\mu_i^{(t+1)} - \bar{\mu}_i^{(t+1)}]_d$  is  $O(\epsilon^2)$ , for all  $d$ .*

*Proof.* Let  $\eta_i^{(t)}$  and  $\mu_i^{(t)}$  be the pre-update natural and mean parameters of  $\tilde{p}_i(t)$  respectively. Furthermore, let

$$\begin{aligned} \mu_i^{(t)'} &= \mu_i^{(t)} - \epsilon \left( \nabla A(\theta_0 + \sum_j \lambda_j) - \mathbb{E}_{p_i(z)}[s(z)] - \xi_i \right) \\ &= \mu_i^{(t)} - \epsilon \left( \mu_i^{(t)} - \mathbb{E}_{p_i(z)}[s(z)] - \xi_i \right), \end{aligned} \quad (39)$$

be the mean parameters of  $\tilde{p}_i^{(t)}$  after an EP- $\mu$  update (12) but *before* being mapped to mean parameters of  $\tilde{p}_i^{(t)}$  through (9).  $\xi_i$  is some zero-mean noise, e.g. due to MC variation. The second equality follows from the definition  $\mu_i^{(t)} = \mathbb{E}_{\tilde{p}_i^{(t)}(z)}[s(z)]$ , and the fact that  $\tilde{p}_i^{(t)} = p$  before an update. Now apply map (9) to convert to mean parameters of  $\tilde{p}_i^{(t+1)}$ ,

$$\begin{aligned} \mu_i^{(t+1)} &= \left( \nabla A \circ \eta_i^{(t+1)} \circ (\eta_i^{(t)})^{-1} \circ \nabla A^* \right) (\mu_i^{(t)'}) \\ &= \nabla A \left( \left( \eta_i^{(t+1)} \circ (\eta_i^{(t)})^{-1} \right) \left( \nabla A^* (\mu_i^{(t)'}) \right) \right) \\ &= \nabla A \left( \nabla A^* (\mu_i^{(t)}) + \sum_j \left( \nabla A^* (\mu_j^{(t)'}) - \nabla A^* (\mu_j^{(t)}) \right) \right), \end{aligned} \quad (40)$$

where the last equality is obtained from the definition of  $\eta_i^{(t)}(\cdot)$  for  $\alpha = 1$ , and using

$$\begin{aligned} \lambda_j^{(t+1)} - \lambda_j^{(t)} &= \eta_j' - \eta_j \\ &= A^* (\mu_j^{(t)'}) - \nabla A^* (\mu_j^{(t)}), \end{aligned} \quad (41)$$

for all  $j$ . Substituting in the definition of  $\mu_j^{(t)'}$ , we have

$$\begin{aligned} \mu_i^{(t+1)} &= \nabla A \left( \nabla A^* (\mu_i^{(t)}) + \sum_j \left[ \right. \right. \\ &\quad \left. \left. \nabla A^* \left( (1 - \epsilon) \mu_j^{(t)} + \epsilon (\mathbb{E}_{p_j(z)}[s(z)] + \xi_j) \right) - \nabla A^* (\mu_j^{(t)}) \right] \right). \end{aligned} \quad (42)$$

Taking Taylor expansions around  $\epsilon = 0$ , we have

$$\begin{aligned} \mu_i^{(t+1)} &= \mu_i^{(t)} + \epsilon \left[ \nabla^2 A \left( \nabla A^* (\mu_i^{(t)}) \right) \right] \sum_j \frac{\partial}{\partial \epsilon} \left\{ \right. \\ &\quad \left. \nabla A^* \left( (1 - \epsilon) \mu_j^{(t)} + \epsilon (\mathbb{E}_{p_j(z)}[s(z)] + \xi_j) \right) \right\} \Big|_0 + O(\epsilon^2) \\ &= \mu_i^{(t)} + \epsilon \left[ \nabla^2 A \left( \nabla A^* (\mu_i^{(t)}) \right) \right] \left[ \nabla^2 A^* (\mu_i^{(t)}) \right] \sum_j \frac{\partial}{\partial \epsilon} \left\{ \right. \\ &\quad \left. (1 - \epsilon) \mu_j^{(t)} + \epsilon (\mathbb{E}_{p_j(z)}[s(z)] + \xi_j) \right\} \Big|_0 + O(\epsilon^2) \\ &= \mu_i^{(t)} + \epsilon \left[ \nabla^2 A \left( \nabla A^* (\mu_i^{(t)}) \right) \right] \left[ \nabla^2 A^* (\mu_i^{(t)}) \right] \sum_j \left( \right. \\ &\quad \left. \mathbb{E}_{p_j(z)}[s(z)] + \xi_j - \mu_j^{(t)} \right) + O(\epsilon^2). \end{aligned} \quad (43)$$

Finally, subtract the noise free  $\bar{\mu}_i^{(t+1)}$ , and take expectations (over  $\xi_j$  for  $j = 1, \dots, m$ ) to obtain the bias

$$\mathbb{E} \left[ \mu_i^{(t+1)} - \bar{\mu}_i^{(t+1)} \right] = \mathbb{E} \left[ \epsilon \left[ \nabla^2 A \left( \nabla A^* (\mu_i^{(t)}) \right) \right] \left[ \nabla^2 A^* (\mu_i^{(t)}) \right] \sum_j \xi_j + O(\epsilon^2) \right]. \quad (44)$$

By assumption  $E[\xi_j] = \mathbf{0} \forall j$ , hence the first order term disappears, and the bias is  $O(\epsilon^2)$ .

To see that the expected decrease in  $L$  is also  $O(\epsilon)$ , note that we are simply following the gradient in  $L$  with respect to  $\mu$ , multiplied by the inverse Fisher and scaled by  $\epsilon$ . Neither the reparameterisation (from  $\lambda_i$  to  $\mu_i$ ) or the Fisher depend on  $\epsilon$ , and so the change in  $L$  must be  $O(\epsilon)$  as  $\epsilon \rightarrow 0^+$  by simple Taylor expansion arguments.  $\square$

## G Computational cost analysis

Let  $c_{\text{samp}}$  be the cost of drawing a single sample from one of the tilted distributions. Let  $c_{\text{fwd}}$  be the cost of converting from natural to mean parameters in the base family  $\mathcal{F}$  (the forward mapping). Similarly, let  $c_{\text{bwd}}$  be the cost of converting from mean to natural parameters in  $\mathcal{F}$  (the backward mapping). Recall that  $m$  is the number of sites. We now state the computational complexity of a round of parallel updates in each of the EP variants evaluated in this paper.

**EP** EP draws  $n_{\text{samp}}$  samples from each of the  $m$  sites. It then performs  $m$  backward mappings, to map from moments back to updated site parameters. The total cost is then  $O(mn_{\text{samp}}c_{\text{samp}} + mc_{\text{bwd}})$

**EP- $\eta$**  EP- $\eta$  draws  $n_{\text{samp}}$  samples from each of the  $m$  sites. Each update also involves one forward mapping per iteration. In addition, each iteration also requires  $m$  JVPs through the backward mapping  $\nabla A^*(\cdot)$ . The primals of this JVP are the same for each site, so the linearisation only needs to be performed once per update, costing  $O(2c_{\text{bwd}})$ , but we have  $m$  cotangents. The overall cost of an EP- $\eta$  iteration is therefore  $O(mn_{\text{samp}}c_{\text{samp}} + c_{\text{fwd}} + (2 + m)c_{\text{bwd}})$ .

**EP- $\mu$**  EP- $\mu$  draws  $n_{\text{samp}}$  samples from each of the  $m$  sites. Each update involves one forward mapping, and  $m$  backward mappings per iteration, but notably does *not* require any JVPs. The overall cost of an EP- $\mu$  iteration is therefore  $O(mn_{\text{samp}}c_{\text{samp}} + c_{\text{fwd}} + mc_{\text{bwd}})$ .

**SNEP** SNEP draws  $n_{\text{samp}}$  samples from each of the  $m$  sites, and performs  $m$  backward mappings per iteration. The total cost is then  $O(mn_{\text{samp}}c_{\text{samp}} + mc_{\text{bwd}})$ , which is the same as EP.

In this work we largely assume that  $c_{\text{samp}}$  is the dominant cost. For example, in the NUTS sampler with default numpyro settings, (as used in our experiments), each sample can involve evaluating up to 1024 gradients of the tilted distribution log density.

The other costs,  $c_{\text{fwd}}$  and  $c_{\text{bwd}}$ , depend on  $\mathcal{F}$ . In the case of a MVN family with dense covariance, the forward and backward mappings are  $O(d^3)$ , for  $d$  the dimensionality of  $z$ . When  $d$  is large,  $c_{\text{fwd}}$  and  $c_{\text{bwd}}$  become more significant, in which case the balance will shift in favour of using more samples per update (and taking larger steps). When  $d$  is very large, however, it may be necessary to choose a diagonal covariance base family instead, in which case the mappings can be performed in  $O(d)$  time. Also note that when  $d$  increases,  $c_{\text{samp}}$  will also typically increase at a rate faster than  $d$ , even with optimal tuning [6]. In the main experiments, we used just a single sample per update for EP- $\eta$  and EP- $\mu$ , and they significantly outperformed the baselines when measure in both NUTS steps *and* wall-clock-time.

We also note that the per-iteration cost of  $c_{\text{fwd}}$  and  $c_{\text{bwd}}$  could be reduced by exploiting the results of previous iterations. For example, in the case of a MVN with dense covariance, the cost of the forward and backward mappings are dominated by matrix inversions. This cost could be significantly reduced by using the result from the previous iteration to warm-start a Newton-style iterative inversion routine. This approach was used by Anil et al. [2] to reduce the cost of computing inverse matrix roots as part of a wider deep learning optimisation scheme. We did not make use of such optimisations in our experiments.

## H Experiment details

In this appendix, we give details about the experiments presented in Section 4. To evaluate the performance of the different variants, we monitored KL divergence to an estimate of the optimum, obtained by running EP to convergence with a large number of samples ( $n_{\text{samp}} = 10^5$  for the final iterations). We used 500 different hyperparameter settings for each variant, chosen using random search, and repeated each run using 5 different random seeds, which were used to seed the MCMC samplers. Hyperparameter settings that failed in any of the 5 runs were discarded. We used this setup for all experiments in Section 4.

The  $x$ -axis in Figure 2 of Section 4 corresponds to the number of NUTS steps, or more specifically, the number of NUTS candidate evaluations. This number is hardware and implementation agnostic, and roughly corresponds to the total computational cost incurred up to that point. Wall-clock time results are given in Appendix J.

**Hyperparameter search spaces** For EP, the step size ( $\alpha$ ) was drawn log-uniformly in the range  $(10^{-4}, 1)$ .  $n_{\text{samp}}$  was drawn log-uniformly between  $[d + 2.5, 10000.5)$  and then rounded to the nearest integer, where  $d$  is the dimensionality of  $z$ ; note that the debiasing estimator used by Xu et al. [47] for MVN families is not defined for  $n_{\text{samp}} \leq d + 2$ . The thinning ratio was drawn uniformly from  $\{1, 2, 3, 4\}$ . For EP- $\eta$  and EP- $\mu$ , the step size ( $\epsilon$ ) was drawn log-uniformly in the range  $(10^{-5}, 10^{-2})$ , and  $n_{\text{samp}}$  was fixed to 1. For SNEP, the step size was drawn log-uniformly in the range  $(10^{-5}, 10^{-2})$ .  $n_{\text{samp}}$  and  $n_{\text{inner}}$  were (independently) drawn log-uniformly in the range  $[.5, 10.5)$  and then rounded to the nearest integer.

**Double-loops** All the methods considered can be used in a double-loop manner by taking  $n_{\text{inner}} > 1$  inner steps per outer update. We did not find this necessary in any of our experiments, and so we fixed  $n_{\text{inner}} = 1$  for EP, EP- $\eta$  and EP- $\mu$ . For SNEP we included  $n_{\text{inner}}$  in the search space (as described above) to make sure that setting it to 1 was not negatively impacting its performance.

**Hardware** All experiments were executed on 76-core Dell PowerEdge C6520 servers, with 256GiB RAM, and dual Intel Xeon Platinum 8368Q (Ice Lake) 2.60GHz processors. Each individual run was assigned to a single core.

**Software** Implementations were written in JAX [5], with NUTS [24] used as the underlying sampler. We used the numpyro [38] implementation of NUTS with default settings. For experiments with a NIW base family we performed mean-to-natural parameter conversions using the method of So [41], with JAXopt [4] used to perform implicit differentiation through the iterative solve.

**Sampling hyperparameter adaptation** We performed regular warmup phases in order to adapt the samplers to the constantly evolving tilted distributions, consistent with prior work [47, 44]. The frequency and duration of these warmup phases was also included in the hyperparameter search as follows. We drew the duration (number of samples) of each warmup phase log-uniformly in the range  $[99.5, 1000.5)$  and then rounded to the nearest integer. We then drew the sampling-to-warmup ratio log-uniformly in the range  $(1, 4)$ . This ratio then determined how frequently the warmup was performed, which we rounded to the nearest positive integer number of updates. Note that the Pareto frontier plots in Figures 2 and 6 include the computation/time spent during warmup phases.

**Site parameter initialisation** For EP, EP- $\eta$  and EP- $\mu$ , we initialised the site parameters to  $\lambda_i = \mathbf{0} \forall i$  for all models, with the exception of the cosmic radiation model for reasons we discuss later. SNEP is not compatible with improper site potentials, and so for models where  $\mathcal{F}$  was MVN we used  $\lambda_i = (2m)^{-1}\theta_0 \forall i$ , consistent with Vehtari et al. [44]. Unfortunately this initialisation strategy for SNEP is not always valid when  $\mathcal{F}$  is NIW. This is because the site potentials in SNEP are restricted to being proper distributions, and this constraint was violated when using this initialisation in our experiments. We tried various other initialisation strategies, but none produced satisfactory results or allowed us to make a meaningful comparison, hence we omitted SNEP from the experiments with NIW  $\mathcal{F}$ ; namely, the political survey hierarchical logistic regression and neural response model experiments.

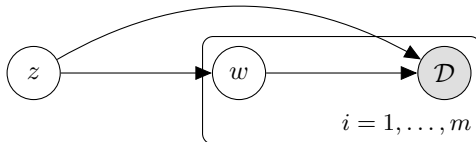


Figure 3: Directed graphical model for the experiments of Section 4.

We set  $\beta_i = 1 \forall i$  in all experiments, corresponding to the original (not power) EP of Minka [33]. All of the models in these experiments followed the same general structure, given by

$$p_0(z) \prod_{i=1}^m p(w_i | z) p(\mathcal{D}_i | w_i), \quad (45)$$

where  $p_0$  is a member of a tractable, minimal exponential family  $\mathcal{F}$ . This is shown graphically in Figure 3. We now provide details about individual experiments.

### H.1 Hierarchical logistic regression

In these experiments, there were  $m$  logistic regression problems, each with  $n$  covariate/response pairs, so that  $\mathcal{D}_i = \{(x_{i,j}, y_{i,j})\}$ ,  $x_{i,j} \in \mathbb{R}^d$ , and  $y_{i,j} \in \{0, 1\}$ . Each regression problem had its own (unobserved) vector of regression coefficients  $w_i \in \mathbb{R}^d$ , with prior density  $p(w_i | z)$  parameterised by global parameters  $z$ .

**Synthetic data with MVN prior** In the synthetic experiment, we had  $m = 16$  regression problems with  $d = 4$  and  $n = 20$ .  $\mathcal{F}$  was the family of MVN distributions, and  $z = (\mu_1, \log \sigma_1^2, \dots, \mu_4, \log \sigma_4^2) \in \mathbb{R}^8$  corresponded to the means and log-variances for the independent normal prior with density  $p(w_i | z) = \prod_{j=1}^4 \mathcal{N}(w_{i,j} | \mu_j, \sigma_j^2)$ .<sup>8</sup> The prior on  $z$  had density  $p_0(z) = \mathcal{N}(\mathbf{0}, \text{diag}((4, 2, 4, 2, \dots)))$ , where  $\text{diag}(\cdot)$  constructs a diagonal matrix from its vector-valued argument. The dataset was generated using the same procedure as Vehtari et al. [44].

**Political survey data with NIW prior** In the political survey data experiment,  $\mathcal{F}$  was the family of normal-inverse-Wishart (NIW) distributions, and  $z = (\mu, \text{vech}(\Sigma))$  was used to parameterise the group-level coefficient prior with density  $p(w_i | z) = \mathcal{N}(w_i | \mu, \Sigma)$ .  $p_0$  was a NIW prior on  $\mu$  and  $\Sigma$ , with parameters  $\mu_0 = \mathbf{0}$ ,  $\nu = 9$ ,  $\lambda = 1$ , and  $\Psi = I$  (following Wikipedia notation). We used a log-Cholesky parameterisation of  $\Sigma$  for the purposes of sampling. The dataset consisted of binary responses to the statement "Allow employers to decline coverage of abortions in insurance plans (Support / Oppose)". We constructed  $m = 50$  regression problems, corresponding to the 50 US states, and truncated the data so that there were exactly  $n = 97$  responses for each state. We used 6 predictor variables from the dataset, corresponding to characteristics of a given survey participant. The predictors were binary variables conveying: age (3 groups), ethnicity (2 groups), education (3 groups) and gender. We also included a state-level intercept to capture variation in the base response level between states, so that  $d = 7$ . This setup is based on one used by Lopez-Martin et al. [29]. The data is available at <https://github.com/JuanLopezMartin/MRPCaseStudy>.

### H.2 Cosmic radiation model

In this experiment, there were  $m$  nonlinear regression problems, each corresponding to a model of the relationship between diffuse galactic far ultraviolet radiation (FUV) and 100- $\mu\text{m}$  infrared (i100) emission in a particular section of the observable universe.

Each nonlinear regression model was parameterised by parameters  $w_i \in \mathbb{R}^9$ . The  $m$  regression problems were related through common hyperparameters  $z \in \mathbb{R}^{18}$ , which parameterised the section-level densities  $p(\mathcal{D}_i, w_i | z)$  where  $\mathcal{D}_i$  is the observed data for sector  $i$ .  $\mathcal{F}$  was the family of MVN distributions, and the prior on  $z \in \mathbb{R}^{18}$  had density  $p_0(z) = \mathcal{N}(\mathbf{0}, 10I)$ . The specifics of  $p(\mathcal{D}_i, w_i | z)$  are quite involved and we refer the reader to Vehtari et al. [44] for further details.

<sup>8</sup>Note that in this section we use  $\mu$  to denote the mean of a normal or multivariate normal distribution. This should not to be confused with the usage for exponential family mean parameters in the main text.

Vehtari et al. [44] applied this model to data obtained from the Galaxy Evolution Explorer telescope. We were unable to obtain the dataset, and so we generated synthetic data using hyperparameters parameters that were tuned by hand to try and match the qualitative properties of the original data set (see Appendix K for examples). We used a reduced number of  $m = 36$  sites and  $n = 200$  observations per site to reduce computation, allowing us to perform a comprehensive hyperparameter search.

Using the conventional site parameter initialisation of  $\lambda_i = \mathbf{0} \forall i$  resulted in most runs of EP failing during early iterations. We found that this was resolved by initialising with the method used by Vehtari et al. [44] for SNEP, that is,  $\lambda_i = (2m)^{-1}\theta_0 \forall i$ , and so we used this initialisation for all methods. We note, however, that the performances of EP- $\eta$  and EP- $\mu$  were largely unaffected by this change.

### H.3 Neural response model

In this experiment we performed inference in a hierarchical Bayesian neural response model, using recordings of V1 complex cells in an anaesthetised adult cat. 10 neurons in a specific area of cat V1 were simultaneously recorded under the presentation of 18 different visual stimuli, each repeated 8 times, for a total of 144 trials. Neural data were recorded by Tim Blanche in the laboratory of Nicholas Swindale, University of British Columbia, and downloaded from the NSF-funded CRCNS Data Sharing website <https://crcns.org/data-sets/vc/pvc-3> [3].

In this experiment  $\mathcal{F}$  was the family of NIW distributions.  $z = (\mu, \text{vech}(\Sigma)) \in \mathbb{R}^{65}$  was used to parameterise  $\mathcal{N}(\log r_j; \mu, \Sigma)$ , the prior distribution density for latent log firing rates in trial  $j$ , for  $j = 1, \dots, 144$ .  $p_0$  was NIW with parameters  $\mu_0 = \mathbf{1}$ ,  $\nu = 12$ ,  $\lambda = 2.5$ , and  $\Psi = 1.25I$  (again following Wikipedia notation). The observed spike count for neuron  $k$  in trial  $j$ ,  $x_{j,k} \in \mathbb{N}$ , was modelled as  $\text{Poisson}(c_{j,k}, \exp(r_{j,k}))$ , for  $j = 1, \dots, 144$ ,  $k = 1, \dots, 10$ . We again used a log-Cholesky parameterisation of  $\Sigma$  for sampling.

We grouped trials together into  $m = 8$  batches of  $n = 18$  trials, so that  $w_i = (\log r_{(i-1)180+1}, \dots, \log r_{(i-1)180+180}) \in \mathbb{R}^{180}$  was the concatenation of (log) firing rates for all 10 neurons across 18 trials, with  $\mathcal{D}_i = \{(x_{j,1}, \dots, x_{j,10})\}_{j=(i-1)180+1}^{(i-1)180+180}$  the observed spike counts.

## I Hyperparameter sensitivity

In this appendix, we examine the effect of varying hyperparameters of EP and EP- $\eta$  on the synthetic hierarchical logistic regression experiment of Section 4.1. The results for EP- $\mu$  are similar to those of EP- $\eta$  and so we do not consider it separately here.

**EP** In Figure 4a we show the effect of varying the number of samples used for estimating updates in EP; more accurate regions of the frontier generally require more samples. Figure 4b similarly shows the effect of varying the step size; more accurate regions of the frontier generally correspond to a smaller step size. Finally, Figure 4c shows the effect of varying the thinning ratio  $\tau$ ; more accurate regions of the frontier correspond to more thinning. Together these plots illustrate the difficulty of tuning EP in stochastic settings. Tracing out the frontier is a three-dimensional problem. To achieve the best accuracy within the compute budget used for this experiment, the practitioner would need to set  $400 < n_{\text{samp}} \leq 500$ ,  $0.1 < \alpha \leq 0.3$ , and  $\tau = 2$ ; and any deviation from this would seemingly result in suboptimal accuracy.

**EP- $\eta$**  In Figure 5a we show the effect of varying the number of samples used for estimating updates in EP- $\eta$ ; the frontier is traced out with  $n_{\text{samp}} = 1$ . We note however that the difference between  $n_{\text{samp}} = 1$  and  $n_{\text{samp}} = 10$  is relatively small, and so it may be sensible to choose  $n_{\text{samp}} > 1$  to make efficient use of parallel hardware, or to minimise per-iteration overheads (see Appendix G). Figure 5b similarly shows the effect of varying the step size; with more accurate regions of the frontier corresponding to a smaller step size. This also suggests that in practice it may make sense to set  $\epsilon$  relatively large at first and then gradually decay it to improve the accuracy. Finally, Figure 5c shows the effect of varying  $n_{\text{inner}}$ , the number of inner steps performed per outer update.  $n_{\text{inner}} > 1$  corresponds to using EP- $\eta$  in "double-loop" mode. We did not find it necessary to increase  $n_{\text{inner}}$  above one to obtain convergence in our experiments, but Figure 5c demonstrates that doing so would

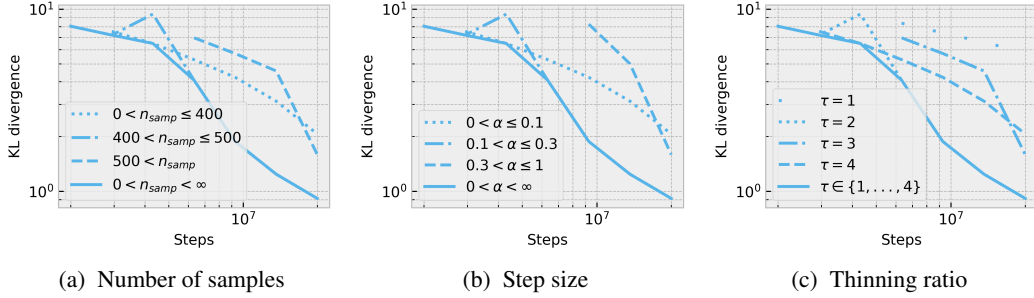


Figure 4: The effect of varying EP hyperparameters; partial Pareto frontiers showing the number of NUTS steps ( $x$ -axis) against the KL divergence from  $p$  to an estimate of the optimum ( $y$ -axis).

have a relatively small impact on performance. Together these plots illustrate that hyperparameter tuning for EP- $\eta$  is relatively straightforward. The frontier can be largely be traced out by varying  $\epsilon$ , and is relatively insensitive to  $n_{\text{samp}}$  and  $n_{\text{inner}}$ .

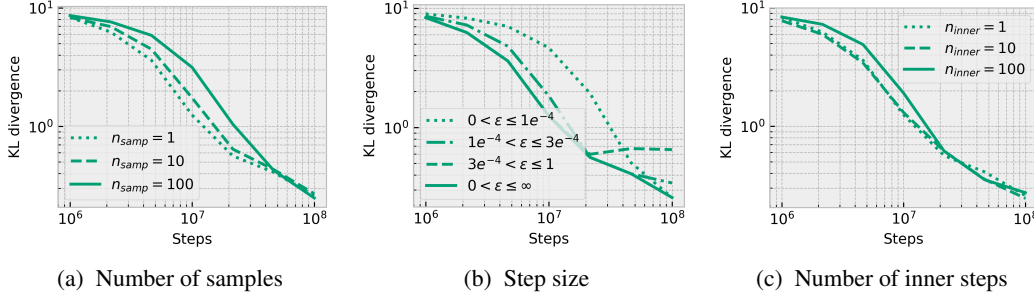


Figure 5: The effect of varying EP- $\eta$  hyperparameters; partial Pareto frontiers showing the number of NUTS steps ( $x$ -axis) against the KL divergence from  $p$  to an estimate of the optimum ( $y$ -axis).

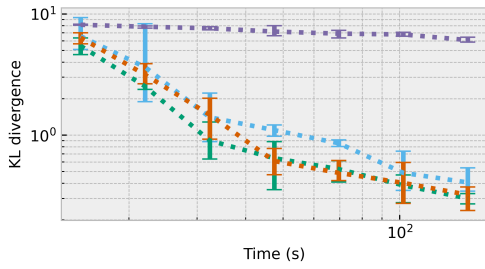
## J Wall-clock time results

In Figure 6, we show Pareto frontiers, with the  $y$ -axis showing the lowest KL divergence achieved by any hyperparameter setting, and the  $x$ -axis shows the cumulative number of seconds elapsed; that is, the wall-clock time equivalent of Figure 2. These results are in broad agreement with those of Figure 2, which suggests the sampling cost does indeed dominate the computational overheads of EP- $\eta$  and EP- $\mu$  in these experiments. The wall-clock time results for EP- $\eta$  and EP- $\mu$  would likely be improved by using more than one sample per update, by making more efficient use of hardware resources and minimising per-iteration overheads.

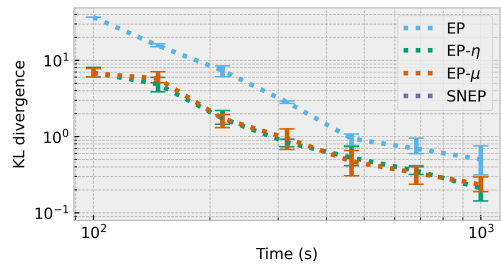
We note that these times are necessarily implementation and hardware dependent. We did not make particular efforts to optimise for wall-clock time. In Appendix G we discuss approaches for minimising per-iteration overheads; these would likely improve wall-clock time performance for all methods, but should disproportionately favour EP- $\eta$  and EP- $\mu$ , due to their frequent updates and larger per-iteration overheads compared to EP and SNEP.

## K Cosmic radiation data

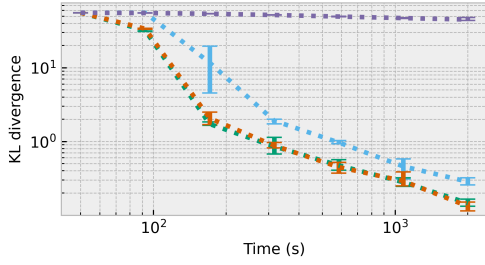
Vehtari et al. [44] used a hierarchical Bayesian model to capture the nonlinear relationship between diffuse galactic far ultraviolet radiation (FUV) and 100- $\mu\text{m}$  infrared emission (i100) in various sectors of the observable universe, using data obtained from the Galaxy Evolution Explorer telescope. We were unable to obtain the dataset, and so we generated synthetic data using hyperparameters parameters that were tuned by hand to try and match the qualitative properties of the original data



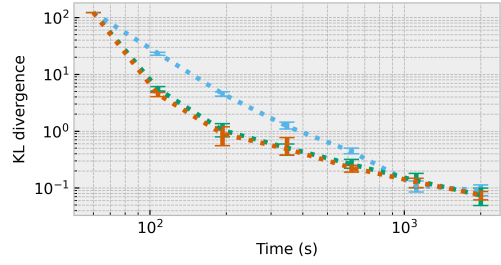
(a) Hierarchical logistic regression: MVN prior



(b) Hierarchical logistic regression: NIW prior



(c) Cosmic radiation model



(d) Neural response model

Figure 6: Pareto frontier showing the number of seconds elapsed ( $x$ -axis) against the KL divergence from  $p$  to an estimate of the optimum ( $y$ -axis). Each point on the plot marks the lowest KL divergence attained by *any* hyperparameter setting by that time. Error bars mark the full range of values for the marked hyperparameter setting across 5 random seeds.

set. Example data generated using these hyperparameters is shown in Figure 7. For comparison, see Figure 9 of Vehtari et al. [44].

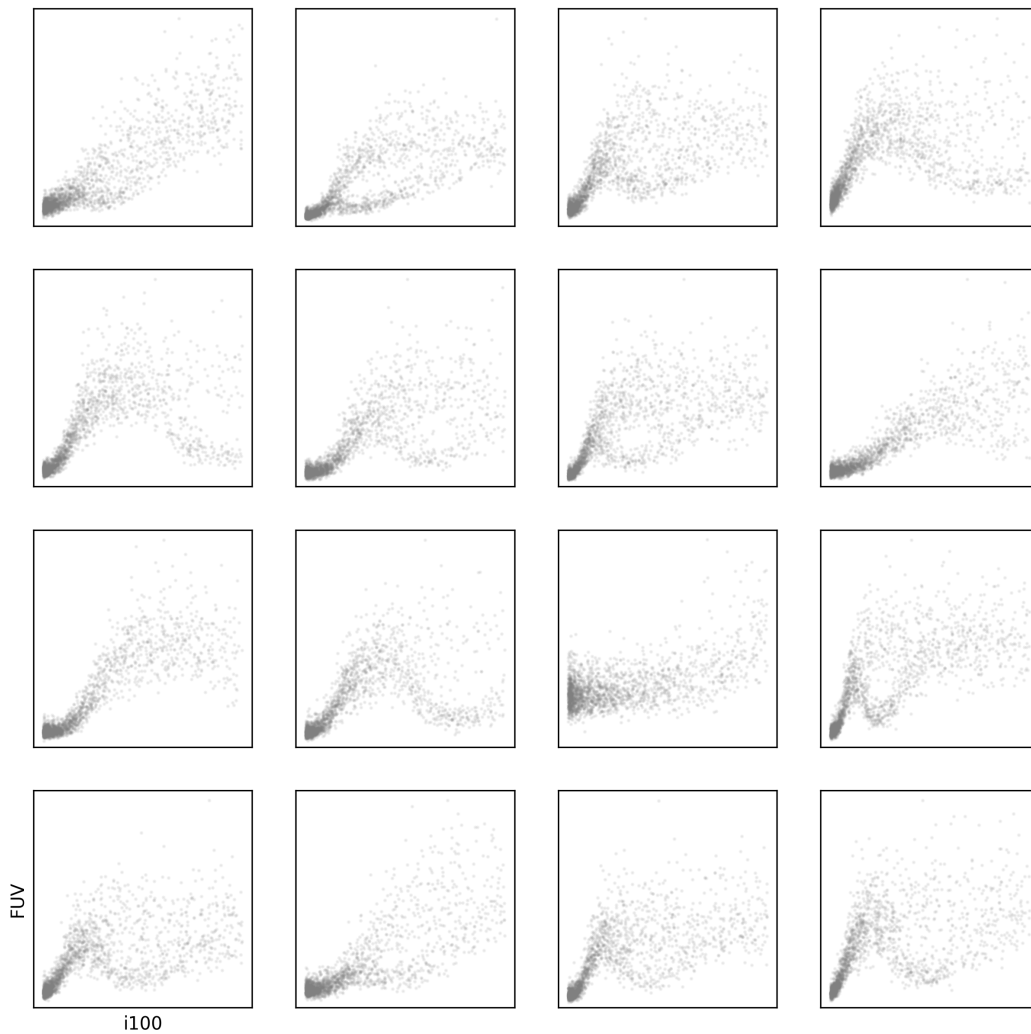


Figure 7: Synthetic data, generated using the cosmic radiation model of Vehtari et al. [44]. Each plot shows galactic far ultraviolet radiation (FUV) versus infrared radiation (i100) for a single sector of the observable universe.